A Novel Terminal Web-Like Structure in Cortical Lens Fibers: Architecture and Functional Assessment

KRISTIN J. AL-GHOUL,[1,2]* TIMOTHY P. LINDQUIST,[1] SPENCER S. KIRK,[1] AND SEAN T. DONOHUE[1]

[1]Department of Anatomy and Cell Biology, Rush University Medical Center, Chicago, Illinois

[2]Department of Ophthalmology, Rush University Medical Center, Chicago, Illinois

ABSTRACT

This study describes a novel cytoskeletal array in fiber cells of the ocular lens of the rat and shows its relationship to the classical terminal web of other epithelial tissues. Naive adult Sprague-Dawley rats (n = 28) were utilized. F-actin, fodrin, myosin IIA, and CP49 distribution was assessed in anterior and posterior polar sections. For functional analysis, lenses were cultured with or without cytochalasin-D for 3 hr, then processed for confocal microscopy or assessed by laser scan analysis along sutures. Phalloidin labeling demonstrated a dense mesh of F-actin adjacent to posterior sutural domains to a subcapsular depth of 400 μm. Anterior polar sections revealed a comparable actin structure adjacent to anterior suture branches however, it was not developed in superficial fibers. Fodrin and myosin were localized within the web-like actin apparatus. The data was used to construct a model showing that the cytoskeletal array is located within the blunt, variable-width fiber ends that abut at sutures such that the "terminal web" flanks the suture on either side. Treatment with cytochalasin-D resulted in partial disassembly of the "terminal web" and perturbed cellular organization. Laser scan analysis revealed that cytochalasin-D treated lenses had significantly greater focal variability than control lenses ($P = 0.020$). We conclude that cortical fibers of rat lenses contain a bipolar structure that is structurally and compositionally analogous to classical terminal webs. The results indicate that the lens "terminal web" functions to stabilize lens fiber ends at sutures thus minimizing structural disorder, which in turn, promotes the establishment and maintenance of lens transparency. Anat Rec, 293:1805–1815, 2010.

Key words: lens; terminal web; cytoskeleton; immunocytochemistry; laser scan analysis

INTRODUCTION

The terminal web is a dense network of cytoskeletal components, located in the cortical region of epithelial cells (Hirokawa and Heuser, 1981). The classical view of the terminal web is that it is apically located, subadjacent to a brush border, and provides an attachment site for actin filament bundles extending from the microvilli of the brush border (Gartner and Hiatt, 2001). It is well-established that the terminal web of intestinal epithelial (brush border) cells contains actin, spectrin, myosin, and intermediate filaments (Mooseker et al., 1978; Hirokawa et al., 1982, 1983; Fath et al., 1993).

Grant sponsor: NIH; Grant number: EY014902.

*Correspondence to: Kristin J. Al-Ghoul, Ph.D., Department of Anatomy and Cell Biology, Rush University Medical Center, 600 S. Paulina St., Ste 507, Chicago, IL 60612. Fax: 312-942-5744. E-mail: kristin_j_al-ghoul@rush.edu

Part of this work was presented at the 2004 ICER Meeting (Sydney, Australia) and the 2006 ARVO Annual Meeting (Ft. Lauderdale, FL).

Timothy P. Lindquist is currently affiliated with Department of Ophthalmology, The University of Kansas, Prairie Village, Kansas

Received 22 February 2010; Accepted 26 April 2010

DOI 10.1002/ar.21216

Published online 20 August 2010 in Wiley Online Library (wileyonlinelibrary.com).

Indeed, these same components are present in the terminal web which underlies apical microvilli in other epithelia, such as kidney brush border cells (Rodman et al., 1986; Al Awqati et al., 1999, 2000) and retinal pigment epithelial cells (Philp and Nachmias, 1985). The cytoskeletal elements of the terminal web are also associated with zonulae adherens on the lateral cell borders; this association is believed to contribute to the stabilization of the apical region both within and between adjacent epithelial cells (Mooseker, 1985; Alberts et al., 2002).

Filamentous terminal web structures are also present in nonbrush border epithelial cells from a variety of tissues, including pancreas, parotid gland, prostate, kidney, and liver (Drenckhahn and Mannherz, 1983; Ishii et al., 1985; Watanabe et al., 1991; Rodriguez et al., 1994; Salas et al., 1997). These nonbrush border terminal web structures contain virtually the same molecular constituents as the terminal web of brush border cells, that is, actin, spectrin, myosin, and intermediate filaments. Significantly, terminal web structures are not always located apically within epithelial cells. In hepatocytes, a terminal web-like structure is located adjacent to the lateral membrane and encircling the bile canaliculi. This pericanalicular plexus is structurally analogous to the apical terminal web of other epithelia, is composed of similar proteins and is associated with zonulae adherens (Ishii et al., 1985; Watanabe et al., 1991). Like the tissues described above, the ocular lens is epithelial-derived and therefore, it may possess similar cytoskeletal arrays.

It is indeed well-established that the cytoskeleton of the lens is comprised of the same three types of filaments found in other (eukaryotic) tissues, namely microfilaments, microtubules, and intermediate filaments. Collectively, the cytoskeletal filaments (and their associated proteins) determine cell shape, polarity, and intracellular organization during differentiation, elongation, and maturation of the lens fiber cells [for review see (Quinlan and Prescott, 2004)]. Whereas the tubulin and actin isoforms found in lens fibers are common to many cell types (Ramaekers et al., 1980; Schmitt-Graff et al., 1990), the two predominant intermediate filament proteins are lens-specific (Gounari et al., 1993; Hess et al., 1993; Merdes et al., 1993). Together, these two proteins, CP49 and filensin (Ireland and Maisel, 1984a,b; Gounari et al., 1993; Hess et al., 1996), form the distinctive beaded filament network in lens fibers [for review see (Fitzgerald, 2009)].

The distribution of cytoskeletal components in lens fibers varies considerably during their differentiation from epithelial cells to mature fibers (Rafferty and Goossens, 1978; Rafferty and Scholz, 1989; Sandilands et al., 1995; Bassnett et al., 1999; Lee et al., 2000; Fischer et al., 2000; Al-Ghoul et al., 2003). This is especially apparent at the apical and basal fiber ends which migrate along the epithelium anteriorly and the capsule posteriorly during fiber elongation and thus, have a specialized cytoskeletal apparatus to perform this function (Bassnett et al., 1999; Lu et al., 2008). At the completion of elongation, fiber ends abut and interdigitate with opposing ends to form the lens sutures [for review see (Kuszak et al., 2004)]. However, the exact basis for the interaction and/or adhesion of fiber ends at sutures remains unknown (Bassnett and Beebe, 2004; Lu et al., 2008). Therefore, we conducted the present study to determine if the cytoskeleton plays a role in the organization of fiber ends at lens sutures. Our results indicate that in rat lenses, a novel cytoskeletal assembly which is structurally analogous to the terminal web of other cell types is present.

MATERIALS AND METHODS

Lenses

A total of 28 normal, Sprague-Dawley rats were utilized in this investigation. All animals were handled in compliance with the ARVO Statement for the Use of Animals in Ophthalmic and Vision Research and with Rush University Medical Center's Institutional Animal Care and Use Committee (IACUC) guidelines. Animals were euthanized by intraperitoneal injection of Euthosol™ and the eyes were enucleated immediately. Lenses were excised and photographed under a stereoscopic zoom microscope (Nikon SMZ1500) and photographed with a digital camera (Nikon DIX, Nikon, Melville, NY) operated by the Q Capture Pro software (QImaging Corporation, Surrey, Canada) on a PC.

Fixation and Vibratome Sectioning

Lenses were fixed in 3% paraformaldehyde in 0.07 M PBS for 2 hr. Fixed lenses were mounted on a sectioning chuck using cyanoacrylate glue and then embedded in warm 2% agar, which solidified at room temperature. To obtain anterior polar sections, the posterior lens surface was adhered to the sectioning chuck and to obtain posterior polar sections, the anterior lens surface was adhered to the sectioning chuck. Polar sections, routinely 100-μm thick, were cut parallel to the lens equator using a vibrating knife microtome (Vibratome-3000 Series, Vibratome, St. Louis, MO) at an amplitude of 3 and a speed of 5 (~0.6 mm/sec). Sections were fixed for an additional 30 min in 3% paraformaldehyde, briefly washed in 0.07 M PBS, and then processed for immunocytochemistry.

Antibodies and Fluorophores

Rabbit polyclonal antibody to (nonmuscle) myosin IIA (M 8064; Sigma Chemical Company, St. Louis, MO) was utilized at a 1:100 dilution. Mouse anti-fodrin monoclonal antibody was used at a 1:200 dilution (MAB1685; Chemicon International, Temecula, CA). Goat anti-CP49 polyclonal antibody was used at 1:200 dilution (sc-67758; Santa Cruz Biotechnology, Santa Cruz, CA). The excitation/emission (ex/em) values for all fluorophores are specified. Phalloidin-FITC (ex/em = 495 nm^3/513 nm^3; Sigma Chemical Company, St. Louis, MO) and phalloidin-TRITC (ex/em = 540–545 nm^3/570–573 nm^3; Sigma Chemical Company, St. Louis, MO) were utilized to label F-actin at a dilution of 1:100 of a methanolic stock (200 U/mL) solution. Wheat germ agglutinin-Alexa Fluor 594 (ex/em = 590 nm^3/617 nm^3; Molecular Probes, Eugene, OR) was used at a dilution of 1:200 in PBS. Secondary antibodies were utilized at a dilution of 1:100 or 1:200 and included: goat anti-rabbit-TRITC and goat anti-rabbit-FITC (both from Sigma Chemical Company, St. Louis, MO; ex/em values as specified above), rabbit anti-

mouse-FITC and rabbit anti-mouse TRITC (both from Sigma Chemical Company, St. Louis, MO; ex/em values as specified above), donkey anti-goat-TRITC (ex/em = 550 nm^3/570 nm^3; Jackson ImmunoResearch, West Grove, PA).

Localization Studies

Immunolabeling was performed by sequentially immersing sections in drops of solution as follows. Sections were permeabilized in 0.2% Triton X-100 for 30 min followed by a 1-hr incubation in a blocking solution of 1% bovine serum albumin (BSA), 0.05% thimerosal and 10% normal serum (goat serum for myosin IIA labeling; rabbit serum for fodrin labeling; donkey serum for CP49 labeling) in 0.07 M PBS. The sections were then incubated overnight at 4°C in the primary antibody diluted as specified above. Appropriate primary antibody dilutions were determined by dilution series tests; dilutions were made in the blocking solution. Following three 10-min washes in blocking solution, sections were incubated in an appropriate secondary antibody conjugated to a fluorescent label for at least 2 hr at room temperature. Sections were washed 4 × 10 min in 0.07 M PBS then mounted between glass slides and cover slips (Gold Seal Products, Portsmouth, NH) with Vectashield mounting medium (Vector Laboratories, Inc., Burlington, CA) to prevent photo bleaching and sealed with lacquer. Specimens were examined on either a Zeiss LSM 510 or Zeiss LSM 510 Meta laser scanning confocal microscope (Carl Zeiss, Göttingen, Germany). Because CP49 and filensin are both required for beaded filament assembly in lens fibers (Sandilands et al., 1995) only one component, CP49, was labeled to determine the distribution of lens-specific intermediate filaments in the present study.

F-actin was localized using fluorescent-labeled phalloidin as follows: Fixed lens sections were permeabilized in 0.2% Triton X-100 for 30 min, and then incubated in phalloidin conjugated to either FITC or TRITC for 30 min. Labeled sections were washed 4 × 10 min in 0.07 M PBS, mounted and examined via confocal microscopy as detailed above.

Control experiments were conducted to ascertain whether the fluorescence was specific binding or nonspecific background. Lenses were fixed and processed as described above. However, normal (nonimmune) serum from the same species in which the primary antibody was raised was utilized in place of the primary antibody as follows: for myosin labeling, sections were treated with normal rabbit serum; for fodrin labeling, antibody was substituted with normal mouse serum; for CP49 labeling, normal goat serum was used. Following the incubations, the specimens were processed, and viewed as described above. In addition, as a positive control for fodrin and CP49 labeling at basal fiber ends, equatorial lens sections were collected and labeled (for either fodrin or CP49) to confirm the expected distribution in fiber cross-sections based on previously published results.

Lens Organ Culture / Cytochalasin-D Treatment

Immediately following euthanasia of rats, lenses were dissected from the eye, placed in culture medium (Minimal Essential Medium with Fetal Bovine Serum, Tryptic Soy Broth, L-glutamine and antibiotics) and incubated at 37°C for 30 min to temperature-stabilize the lenses. OD (right eye) lenses received cytochalasin-D at 20 μM and were allowed to incubate for an additional 3 hr. OS (left eye) lenses were incubated for an equivalent time in the above media as untreated controls. After culturing, lenses were evaluated by either laser scan analysis or confocal microscopy.

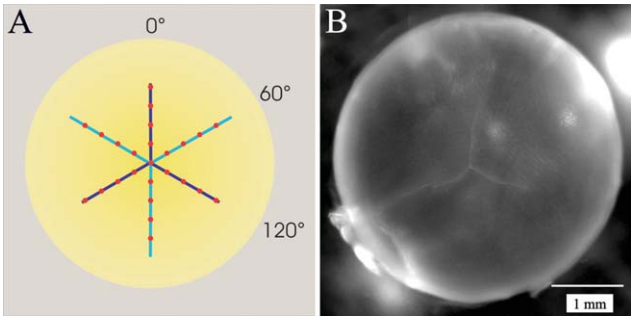

Fig. 1. **A**: Diagram demonstrating the position of laser beam penetrations with respect to the lens sutures. Anterior suture branches are in light blue; posterior suture branches are in dark blue (seen through the lens). Each series of scans passes along an anterior and a posterior suture branch. **B**: Photograph of the posterior aspect of a rat lens showing the typical inverted Y suture pattern.

Laser Scan Analysis

After culturing, the mean back vertex distance (average BVD) was assessed for all lenses using the Scantox™ *In Vitro* Assay System (Harvard Apparatus) as described previously (Kuszak and Al-Ghoul, 2002). Briefly, lenses were placed in specially designed chambers of glass and silicon rubber containing fresh M199 culture media (supplemented with Earle's salts and 8% fetal bovine serum) at 37°C. Care was taken to insure that both anterior and posterior surfaces of the lens were bathed in culture media at all times. Lenses were suspended within the glass chamber on a beveled washer which supported the equatorial rim, and oriented so that lasers pass through the lens as in the anatomical position (anterior to posterior). All lenses were scanned with 3 series of laser beams at 0-degree, 60-degree, and 120-degree angle as shown in Fig. 1A. Each scan series passed along an anterior and posterior suture branch because the anterior and posterior suture patterns are offset by 60-degree angle. Every series of laser scans consisted of nine penetrations at equal increments passed along the lens, resulting in a total of 27 objective measurements per lens. The typical inverted Y suture pattern of the posterior lens surface is demonstrated in Fig. 1B. In the Scantox™ *In Vitro* Assay System, back vertex distance (BVD) is defined as measuring the laser beam from the rear surface of the lens to the focal point (Kuszak et al., 1991, 1994; Sivak et al., 1994). Repeated BVD measurements have previously indicated that instrument reproducibility stays within 0.32% (focal length). Whereas lens focusing *in vivo* is typically influenced by both coma and longitudinal spherical aberration, the changes in BVD with beam position in this *in vitro* system are largely due to longitudinal spherical aberration (Kuszak et al., 1991;

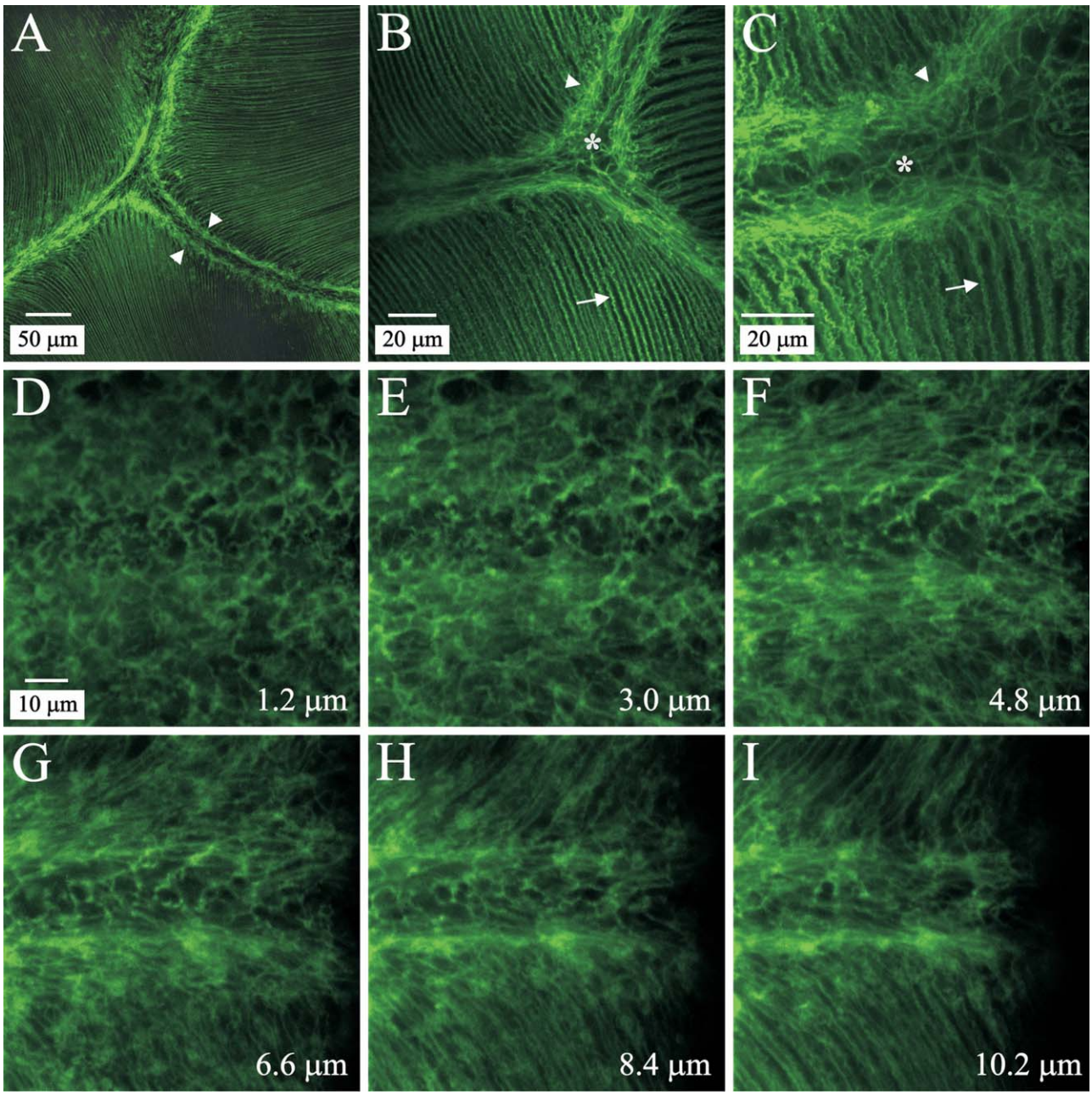

Fig. 2. LSCM images of phalloidin-FITC-labeled posterior polar lens sections. **A**: Low magnification of the confluence of the posterior sutures ~10 μm deep to the CFI. The typical inverted-Y suture pattern is apparent. **B**: Medium magnification of posterior sutures at about 50 μm from the CFI. The sutural region is flanked by the web-like mesh, which appears to attach to the actin filaments in both the fiber ends and the lateral fiber borders. **C**: High magnification of a posterior suture branch ~275 μm deep to the CFI. **D–I**: Nonadjacent optical sections from a z-series taken near the proximal end of a posterior suture branch, showing the formation of the web-like F-actin structure. Distance from the CFI is indicated in the lower right corner of each panel; D–I are at identical magnification. By ~3.5 μm from the CFI an indistinct mesh of F-actin was present flanking the forming suture branch. At 10 μm deep to the CFI, the F-actin underlying lateral fiber membranes is contiguous with the well-formed web-like structure.

Kuszak and Al-Ghoul, 2002). Furthermore, structural irregularities within the lens can cause deviations in the path of individual laser beam penetrations, causing a more scattered appearance of the focal point. Therefore, the variability in BVD was also measured. Variability in BVD is defined as the average standard error of the means of the BVD of all lenses per group.

Data Analysis

Statistical calculations were performed to determine if BVD and variability in BVD were significantly different in cytochalasin-D-treated rat lenses as compared to control lenses. Specifically, the Mann-Whitney (rank-sum) test was utilized. A probability value of $P \leq 0.05$ was considered significant.

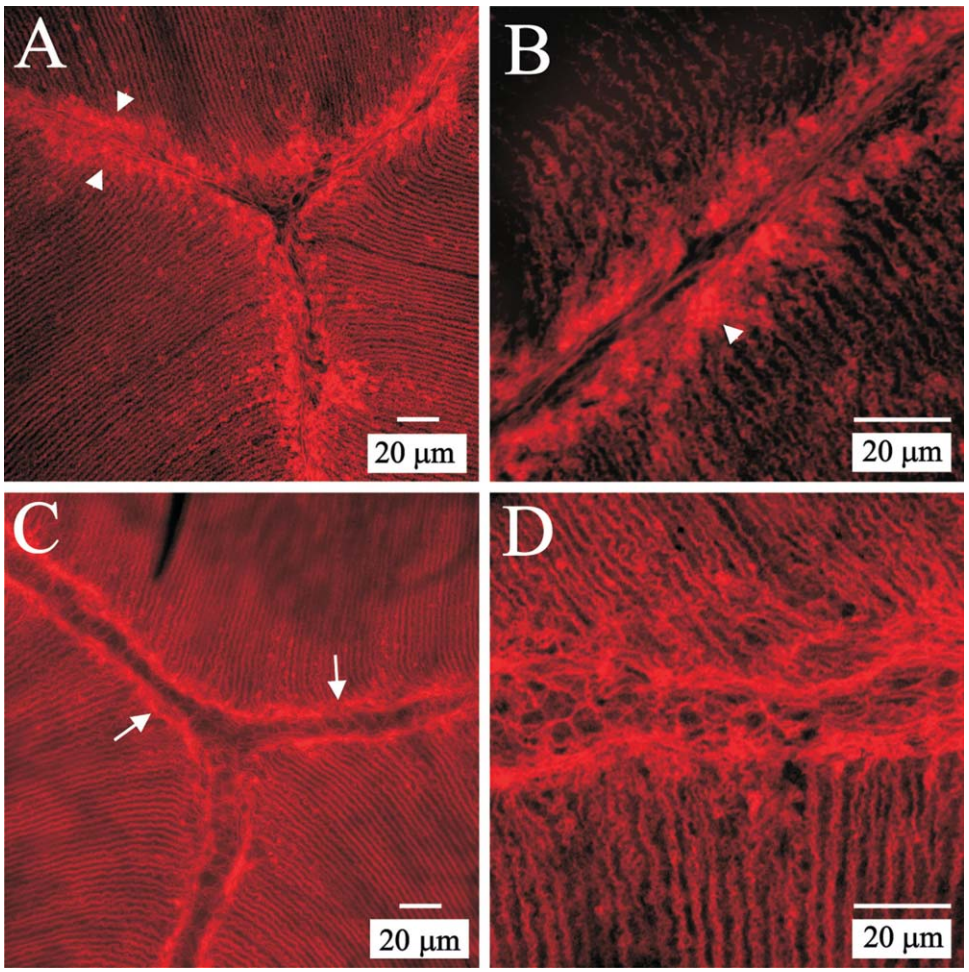

Fig. 3. LSCM images of phalloidin-TRITC labeled anterior polar lens sections. **A**: Low magnification of the confluence of anterior sutures ~10 μm deep to the EFI shows accumulations of F-actin at fiber ends. **B**: Higher magnification of an anterior suture branch in another lens (~15 μm deep to the EFI) reveals that F-actin is not organized into a mesh-like web in anterior ends of superficial maturing fibers. **C**: Low magnification of the confluence of anterior suture branches about 60 μm from to the EFI shows a prominent "terminal web." **D**: Higher magnification of an anterior suture branch in another lens ~75 μm deep to the EFI shows the F-actin web architecture is comparable to that at posterior ends of fibers.

Fiber End Organization After Organ Culture

The morphology and organization of fiber ends was assessed in some lenses after organ culture by fluorescent labeling and LSCM visualization. Briefly, after culturing, control and experimental lenses were fixed and sectioned in the same manner as the localization studies. Tissue sections were double-labeled to visualize the membranes and the actin cytoskeleton with wheat germ agglutinin-TRITC conjugate (Molecular Probes, Eugene, OR) and phalloidin-FITC conjugate, respectively. Labeled sections were mounted and examined as stated above.

RESULTS

Architecture

Phalloidin labeling revealed that a dense mesh of F-actin was present adjacent to, but not within, posterior sutural domains (Fig. 2A–C, arrowheads) in fully elongated lens fibers. As expected, actin labeling also delineated the lateral fiber membranes of posterior fiber segments (Fig. 2B,C, arrows) and was present at sutures where fiber ends abut and interdigitate (Fig. 2B,C, asterisks). Structurally, this web-like mesh was similar to classical epithelial terminal webs in which actin filaments in the surface specialization attach to the terminal web. Specifically, in rat lens fibers, actin filaments in both the interdigitated fiber ends and the lateral membrane domains appeared to attach to the F-actin mesh. Through-focus z-series analysis of posterior polar lens sections ascertained that the terminal web-like apparatus began to form in fiber ends located only a few micrometers deep to the posterior capsule (Fig. 2D–I). In particular, by ~3.5 μm from the capsule–fiber interface (CFI) an indistinct mesh of F-actin was present flanking the forming suture branch (Fig. 2F). At 10 μm from the CFI, cortical F-actin (which underlies the lateral fiber membrane) adjoined the well-formed web-like structure (Fig. 2I). The "terminal web" of lens fibers was observed

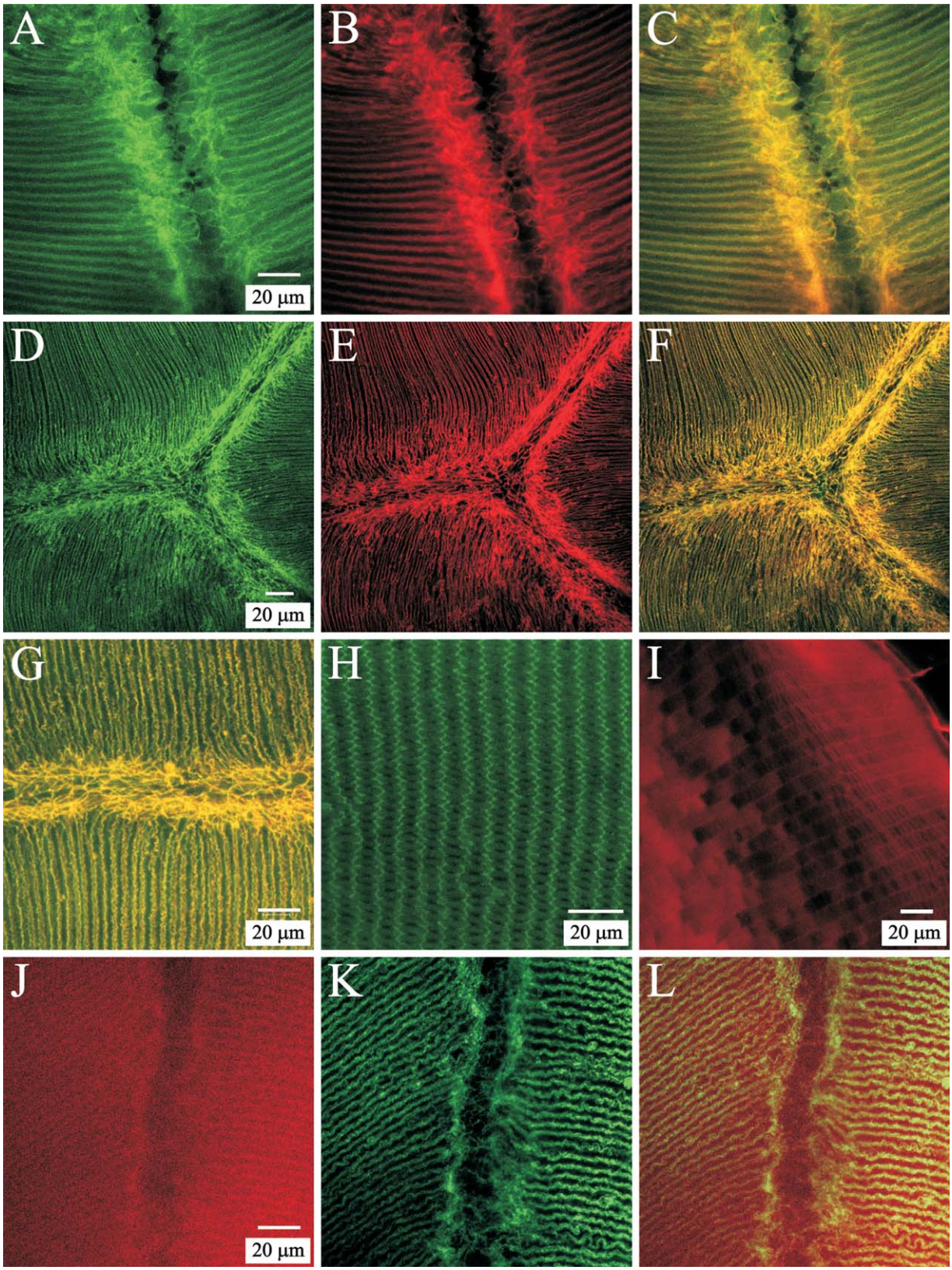

Fig. 4. LSCM localization of terminal web proteins within the F-actin web of lens fibers. **A–C**: Double labeling for myosin (A) and F-actin (B) at a posterior suture branch. The merged image (C) shows that myosin and actin were largely colocalized within the web-like mesh as well as along lateral aspects of fiber segments. Myosin was present in fiber ends as a diffuse plaque (consistent with previously published data (Lu et al., 2008). A–C are at identical magnification. **D–F**: Low-magnification image series of double labeling for fodrin (D) and F-actin (E) in a posterior polar section. The merged image (F) demonstrates a high degree of colocalization. D–F are at the same magnification. **G**: Merged higher magnification view of a posterior suture branch double labeled for fodrin and F-actin shows the extensive colocalization of these components within the "terminal web" as well as along lateral fiber membranes. **H**: Positive control for fodrin specificity. Fodrin localization in equatorial segments of cortical fibers revealed that labeling was most prominent along the short sides of hexagonal fiber profiles. **I**: Positive control for CP49 specificity. Equatorial segments of cortical fibers demonstrated peripheral localization of CP49 in superficial fibers and a more diffuse, cytoplasmic labeling in deeper cortical fibers. **J–L**: Double labeling for CP49 (J) and F-actin (K) at a posterior suture branch revealed the diffuse pattern of CP49 label both within the "terminal web" and along posterior segments of fibers. The merged image (L) emphasizes the lack of strong CP49 labeling within the F-actin web adjacent to the posterior suture branch. J–L are at identical magnification.

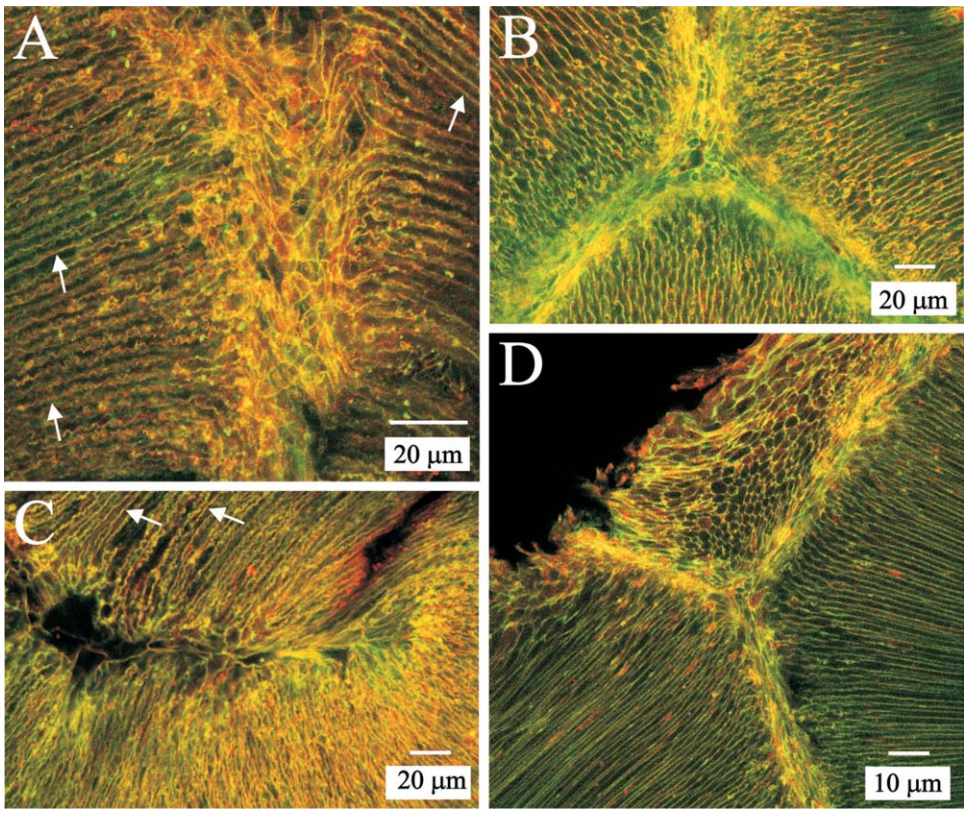

Fig. 5. LSCM visualization of cytochalasin D-treated (**A**,**C**) and control (**B**,**D**) lenses. Panels A and B show posterior sutures at ~20 μm and 40 μm from the CFI, respectively; panels C and D illustrate anterior sutures at about 110 μm and 85 μm from the EFI, respectively. Specimens were double labeled for F-actin (green) and wheat germ agglutinin (red) to localize the actin cytoskeleton and outline the fiber membranes. Cytochalasin D treatment resulted in partial disassembly of the "terminal web" resulting in disarray of fiber end arrangement at both the posterior (A) and anterior (C) sutures. In contrast, fiber end segments outside of the sutural domains were intact and appeared undisrupted by cytochalasin D treatment (arrows).

up to 400-μm deep to the capsule (data not shown). At the anterior ends of fully elongated, superficial fibers, dense accumulations of actin were seen (Fig. 3A,B, arrowheads). However, in all lenses examined, a web-like F-actin mesh had formed by ~50-μm deep to the EFI (Fig. 3C,D, arrows). This "terminal web" was structurally analogous to the web at posterior fiber ends.

Molecular Components of the "Terminal Web"

Because epithelial terminal webs from a variety of tissues all contain actin, spectrin, myosin, and intermediate filaments (Mooseker et al., 1978; Hirokawa et al., 1983; Philp and Nachmias, 1985; Rodman et al., 1986; Fath et al., 1993), we performed immunofluorescent labeling for myosin IIA (nonmuscle), fodrin (nonerythrocyte spectrin), and CP49 (a lens-specific intermediate filament protein) to determine their presence and distribution with respect to the F-action web of lens fibers (Fig. 4). Both myosin IIA (Fig. 4A) and fodrin (Fig. 4D) were strongly localized to the terminal web-like apparatus and showed nearly complete colocalization with F-actin (Fig. 4C, F, and G). However, although labeling for CP49 was present in the region of the web (Fig. 4J), its distribution was quite diffuse and it was not especially abundant within or subadjacent to the F-actin web (Fig. 4L). Negative controls were performed by treating sections with normal (nonimmune) serum from the same species in which the primary antibodies (myosin IIA, fodrin and CP49) were raised. In each case, specimens did not exhibit specific labeling (data not shown).

Positive controls were executed to confirm that the antibodies for fodrin and CP49 gave a comparable distribution to previously published data. Specifically, equatorial sections having cross-sectioned cortical fibers were labeled (separately) for each component. Immunofluorescence for fodrin was prominent along the short-sides of cross-sectioned fiber profiles with faint or no labeling in the center of the long sides (Fig. 4H). This is consistent with data from prior studies (Lee et al., 2000; Nowak et al., 2009) and confirmed the specificity of the fodrin antibody utilized in the present study. Similarly, CP49 was localized at the periphery of fiber profiles in superficial fibers but showed more diffuse cytoplasmic labeling in deeper cortical fibers (Fig. 4I). This result is consistent with previously published results from other investigators (Merdes et al., 1993; Oka et al., 2008) and confirmed the specificity of the commercial antibody we utilized.

Cytochalasin-D Treatment and Laser Scan Analysis

Three hour treatment with 20 μM cytochalasin-D resulted in disruption of fiber end arrangement at

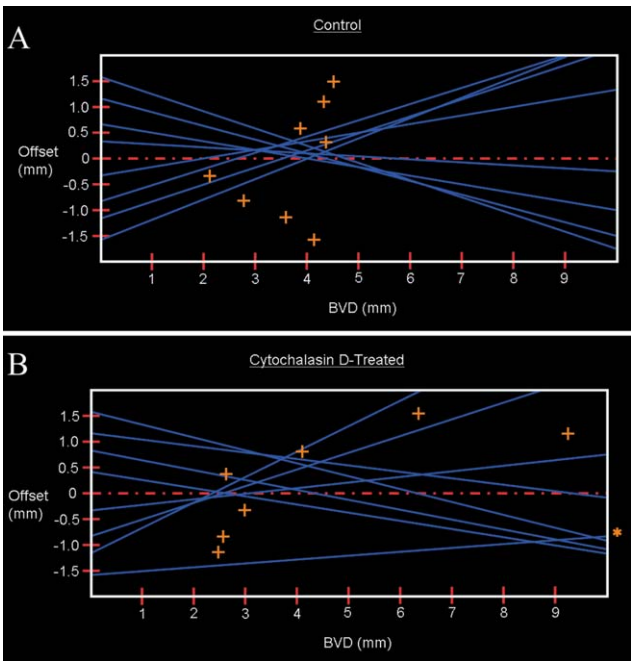

Fig. 6. Representative laser scan profiles of OS lenses **(A)** which were untreated controls and OD lenses **(B)** which were treated with Cytochalasin D. The more diffuse pattern of laser scans for the cytochalasin-D treated lenses illustrates their greater variability in BVD. The offset distance is the distance from the lens center for each scan series. Blue lines represent individual laser beam penetrations; orange crosses denote the BVD for each laser penetration. A: Mean BVD = 3.6 mm. B: Mean BVD = 6.3 mm. Laser penetration at offset −1.5 (indicated by asterisk) had a BVD of 20.3 mm.

sutures (Fig. 5A,C), although the remainder of posterior fiber segments appeared unperturbed (Fig. 5A,C, arrows). Fiber end arrangement and F-actin distribution in untreated (control) lenses appeared comparable to that seen in localization studies (compare Fig. 5B with Fig. 2B and Fig. 5D with Fig. 3C), thus suggesting that short-term culturing did not adversely affect the fiber end structure and/or the architecture of the web-like F-actin apparatus.

Representative laser scan profiles for experimental and control lenses are shown in Fig. 6 and illustrate the functional changes that occurred after short-term (3 hr) organ culture with or without cytochalasin-D treatment in normal juvenile rat lenses. The laser scan data is summarized in Table 1. Laser scan analysis revealed that the sutural domains of cytochalasin D-treated lenses had a greater average BVD than those in untreated contralateral lenses although the difference was not statistically significant ($P = 0.059$). However, the average variability in BVD was significantly greater in treated vs. controls ($P = 0.020$). It should be noted that some (2 of 8) cytochalasin-D treated lenses had an average BVD that was within the same range as the control lenses, indicating a limited response to treatment. Of the two lenses that displayed a limited response to cytochalasin-D treatment, one of these also had a standard error value (variability in BVD) which was within the control range. All other values for variability in BVD were markedly outside the range seen in control lenses (~10-fold increase). The data suggests that other factors may be affecting the individual lens response to short-term cytochalasin-D treatment.

TABLE 1. Back vertex distance (BVD) and variability in back vertex distance in organ cultured rat lenses

Parameter	Cytochalasin D-treated lenses (n = 8)	Control lenses (n = 6)	*P*
Mean BVD ± SEM	7.06 ± 1.18	3.96 ± 0.10	0.059
Median	6.82	3.98	–
Range	3.01–12.24	3.64–4.29	–
Mean variability in BVD ± SEM	3.10 ± 0.54	0.37 ± 0.03	0.020[a]
Median	3.44	0.35	–
Range	0.20–4.64	0.29–0.48	–

n = number of animals.
[a]Indicates a statistically significant difference.

DISCUSSION

It is evident that superficial cortical fibers of rat lenses contain a cytoskeletal assembly that is structurally analogous to the terminal web of other epithelia. The "terminal web" forms in fully elongated fibers which have detached from the capsule and interdigitated with opposing fibers to form sutures. This cytoskeletal array is comparable with apical terminal webs in which actin filaments in the surface specialization attach to the web, providing a stabilizing anchor point (Ross et al., 2003). Specifically, in lens fibers, actin filaments in both the abutted fiber ends and the lateral membrane domains appeared to attach to the F-actin mesh which is adjacent to, but not directly within, the fiber ends. This suggests that the actin web in lens fibers has a comparable role in stabilizing the fiber ends that interdigitate at lens sutures.

In contrast to classical epithelial terminal webs, which are apically located, the lens "terminal web" is a bipolar structure found adjacent to both anterior and posterior fiber ends. This is somewhat similar to the pericanalicular terminal web in hepatocytes, which may be present at 2 or even 3 locations around the cell periphery (Sormunen et al., 1993; Massey-Harroche et al., 1998). Although it is bipolar, the "terminal web" of lens fibers is not well-developed in the most superficial anterior fiber ends, initially manifesting in fibers located 30–40 μm deep to the anterior capsule (as opposed to 10 μm deep to the posterior capsule). Thus, it is evident that it develops at a different rate in anterior versus posterior fiber ends. This is consistent with prior observations that anterior fiber ends migrate at a slower rate than posterior ends (Bassnett and Winzenburger, 2003), resulting in posterior suture development preceding anterior suture development for any given cohort of fibers (Kuszak et al., 2004). Clearly, the anterior and posterior fiber segments develop with a degree of independence which may reflect their differing source of metabolites (aqueous vs. vitreous) and/or the substratum across which the fiber ends migrate (epithelium vs. capsule).

The localization of both myosin and fodrin to the F-actin mesh in lens fibers furthers its analogy to classical terminal webs. In brush border cells, myosin is localized

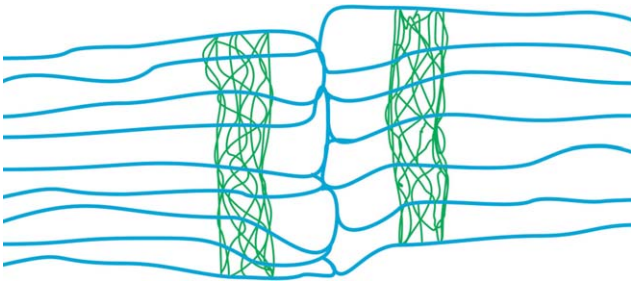

Fig. 7. Two-dimensional model of murine fiber end segment architecture showing the relative position of the "terminal web" within a single growth shell. End segments of fibers (membranes shown in blue) are nonuniform in width and have blunt ends where they abut with opposing fiber ends to form a suture. The F-actin of the web-like cytoskeletal apparatus (shown in green) is located within fiber ends such that the "terminal web" flanks the suture on either side. Neither the undulating surface topology of lateral fiber membranes nor the cortical actin beneath them is depicted.

throughout the filamentous network of the terminal web as well as concentrated near adhering junctions (Drenckhahn and Groschel-Stewart, 1980; Drenckhahn et al., 1980) and is capable of mediating contraction of the terminal web (Rodewald et al., 1976). Terminal web contraction results in subsequent rounding of the apical cell surface and fanning apart of microvilli (Keller and Mooseker, 1982; Burgess, 1982; Keller et al., 1985). However, other studies indicate that myosin also functions as a structural cross-linker which is essential to the maintenance of the actin mesh and the orientation of the overlying microvilli (Hirokawa et al., 1982; Temm-Grove et al., 1992). Given the tightly packed arrangement of maturing lens fibers which restricts fiber end movement, a structural role for myosin within the lens "terminal web" seems most probable. Specifically, myosin could function as a cross-linking element within the actin web as well as with adhering junctions which have been localized to the adjacent lateral cell borders in this cell population (Beebe et al., 2001; Lu et al., 2008). Fodrin, the nonerythrocyte spectrin homologue, was identified in the terminal web of brush border cells more than 25 years ago (Weber and Glenney, 1982; Glenney et al., 1982; Hirokawa et al., 1983) and in that location, it binds to actin and cross-links microfilaments to one another as well as to the plasma membrane (Glenney et al., 1983; Hirokawa et al., 1983; Pearl et al., 1984; Rodman et al., 1986). It is well established that fodrin is a key component in the membrane skeleton of lens fibers (Ireland and Maisel, 1984b; Allen et al., 1987). It binds to cortical actin (Green and Maisel, 1984) and participates in the establishment and maintenance of cell shape and organization during lens fiber differentiation (Fischer et al., 2000; Lee et al., 2000; Woo et al., 2000; Lee et al., 2001; Lu et al., 2008; Nowak et al., 2009). It is likely that fodrin's function in the lens "terminal web" is parallel to its role in the terminal web of brush border cells, that is, it cross-links other cytoskeletal elements and links the entire array to the plasma membrane.

Intermediate filaments typically underlie the actin-spectrin-myosin mesh in an epithelial terminal web, providing additional support for the brush border and tensile strength to the epithelial sheet as a whole (Mooseker et al., 1978; Hirokawa et al., 1982; Hirokawa et al., 1983; Fath et al., 1993). However, this is not the case in lens fibers as the "terminal web" was not specifically associated with the predominant intermediate filament type in the lens, the beaded filaments. This may simply reflect the decreased need for structural reinforcement in the absence of a brush border.

It is well-established that fiber end morphology varies depending on the suture type (branchless versus branched) and on the number of branches present (Kuszak and Brown, 1994). In particular, rat (and mouse) lenses have a three-branched "Y" suture pattern, which necessitates a reduction in fiber width at anterior and posterior ends with respect to the equatorial fiber segment width (Kuszak, 1995). The precise morphology of murine lens fibers at the sutures has been documented in several prior studies (Kuszak, 1995; Al-Ghoul et al., 1998; Kuszak et al., 2006; Shi et al., 2009) all of which showed that terminal portions of fibers were blunt-ended, of variable width and often slightly irregular in shape. Using this prior data, we have constructed a model of fiber end architecture at sutures with respect to the "terminal web" (Fig. 7). From this, it can be seen that the terminal web-like apparatus of rat lens fibers lies within the irregular end segments of fibers as they approach the suture, but not within the most distal portions of the fiber ends. The web is aligned from fiber to fiber, forming a band which appears contiguous both within and between successive cohorts of maturing fibers. Because each suture branch is comprised of two sets of opposing fiber ends, the "terminal web" flanks the suture branches on either side.

As the function of the ocular lens is to focus light onto the retina, lens transparency is a prerequisite for proper function. Prior studies have elucidated that the precise arrangement and packing of lens fibers in a crystalline array contributes to lens transparency (Kuszak and Brown, 1994; Kuszak and Costello, 2004) and conversely, that disruptions or modifications of this fiber arrangement adversely affect lens function (Shiels et al., 2000, 2001; Sandilands et al., 2003). In particular, the lens sutures adversely affect overall focal ability because they are regions of relative disorder within the lens and are situated directly on the visual axes (Kuszak et al., 1991, 1994, 2000; Sivak et al., 1994; Kuszak and Al-Ghoul, 2002). Therefore, it is obvious that maintenance of fiber end order at sutures is vital to the preservation of optimal lens function. In the present study, partial disassembly of the "terminal web" after cytochalasin-D treatment resulted in disorganization of fiber end packing and a significant increase in focal variability as measured by laser scan analysis. This indicates that the "terminal web" provides a mechanism whereby fiber ends maintain their size, shape and relative positions within each growth shell as they abut and interdigitate with opposing fiber ends to form sutures.

Although treatment of organ-cultured lenses with cytochalasin-D would, presumably, affect the actin cytoskeleton throughout fibers, the data did not show a concomitant disruption of cortical actin beneath the lateral fiber membranes or an alteration in fiber packing (Fig. 5A,C). It is likely that cortical actin is stabilized by its association with multiple membrane skeleton components (Fischer et al., 2000; Lee et al., 2000; Nowak et al., 2009) as seen in other tissues (Lux, 1979; Luna and Hitt, 1992).

In summary, the data indicates that lens fibers possess a bipolar "terminal web" that is similar to the classical terminal web of epithelial tissues. This novel cytoskeletal array functions to stabilize fiber ends both within and between growth shells, thus contributing to the maintenance of fiber order at sutures and ultimately, impacting overall lens function.

ACKNOWLEDGMENTS

The authors thank Dr. J. R. Kuszak for the use of his Scantox™ *In Vitro* Assay System and Anita Joy for the creation of the 2D model. The technical assistance of Dana Williams, Joan Kim, and Anita Joy is gratefully acknowledged.

LITERATURE CITED

Al Awqati Q, Vijayakumar S, Takito J, Hikita C, Yan L, Wiederholt T. 1999. Terminal differentiation in epithelia: the Hensin pathway in intercalated cells. Semin Nephrol 19:415–420.

Al Awqati Q, Vijayakumar S, Takito J, Hikita C, Yan L, Wiederholt T. 2000. Phenotypic plasticity and terminal differentiation of the intercalated cell: the hensin pathway. Exp Nephrol 8:66–71.

Al-Ghoul KJ, Kuszak JR, Lu JY, Owens MJ. 2003. Morphology and organization of posterior fiber ends during migration. Mol Vis 9:119–128.

Al-Ghoul KJ, Novak LA, Kuszak JR. 1998. The structure of posterior subcapsular cataracts (PSCs) in the Royal College of Surgeons (RCS) rats. Exp Eye Res 67:163–177.

Alberts B, Johnson A, Lewis J, Raff MC, Roberts K, Walter P. 2002. Molecular biology of the cell. 4th ed. New York: Garland Science.

Allen DP, Low PS, Dola A, Maisel H. 1987. Band 3 and ankyrin homologues are present in eye lens: evidence for all major erythrocyte membrane components in same non-erythroid cell. Biochem Biophys Res Commun 149:266–275.

Bassnett S, Beebe DC. 2004. Lens fiber differentiation. In: Lovicu FJ, Robinson ML, editors. Development of the ocular lens. Cambridge: Cambridge University Press. p 214–244.

Bassnett S, Missey H, Vucemilo I. 1999. Molecular architecture of the lens fiber cell basal membrane complex. J Cell Sci 112 (Part 13):2155–2165.

Bassnett S, Winzenburger PA. 2003. Morphometric analysis of fibre cell growth in the developing chicken lens. Exp Eye Res 76:291–302.

Beebe DC, Vasiliev O, Guo J, Shui YB, Bassnett S. 2001. Changes in adhesion complexes define stages in the differentiation of lens fiber cells. Invest Ophthalmol Vis Sci 42:727–734.

Burgess DR. 1982. Reactivation of intestinal epithelial cell brush border motility: ATP-dependent contraction via a terminal web contractile ring. J Cell Biol 95:853–863.

Drenckhahn D, Groschel-Stewart U. 1980. Localization of myosin, actin, and tropomyosin in rat intestinal epithelium: immunohistochemical studies at the light and electron microscope levels. J Cell Biol 86:475–482.

Drenckhahn D, Mannherz HG. 1983. Distribution of actin and the actin-associated proteins myosin, tropomyosin, alpha-actinin, vinculin, and villin in rat and bovine exocrine glands. Eur J Cell Biol 30:167–176.

Drenckhahn D, Steffens R, Groschel-Stewart U. 1980. Immunocytochemical localization of myosin in the brush border region of the intestinal epithelium. Cell Tissue Res 205:163–166.

Fath KR, Mamajiwalla SN, Burgess DR. 1993. The cytoskeleton in development of epithelial cell polarity. J Cell Sci Suppl 17:65–73.

Fischer RS, Lee A, Fowler VM. 2000. Tropomodulin and tropomyosin mediate lens cell actin cytoskeleton reorganization in vitro. Invest Ophthalmol Vis Sci 41:166–174.

Fitzgerald PG. 2009. Lens intermediate filaments. Exp Eye Res 88:165–172.

Gartner LP, Hiatt JL. 2001. Color textbook of histology. 2nd ed. Philadelphia: W.B.Saunders Co.

Glenney JR, Jr., Glenney P, Osborn M, Weber K. 1982. An F-actin- and calmodulin-binding protein from isolated intestinal brush borders has a morphology related to spectrin. Cell 28:843–854.

Glenney JR, Jr., Glenney P, Weber K. 1983. The spectrin-related molecule, TW-260/240, cross-links the actin bundles of the microvillus rootlets in the brush borders of intestinal epithelial cells. J Cell Biol 96:1491–1496.

Gounari F, Merdes A, Quinlan R, Hess J, Fitzgerald PG, Ouzounis CA, Georgatos SD. 1993. Bovine filensin possesses primary and secondary structure similarity to intermediate filament proteins. J Cell Biol 121:847–853.

Green J, Maisel H. 1984. Lens fodrin binds actin and calmodulin. Curr Eye Res 3:1433–1440.

Hess JF, Casselman JT, Fitzgerald PG. 1993. cDNA analysis of the 49 kDa lens fiber cell cytoskeletal protein: a new, lens-specific member of the intermediate filament family? Curr Eye Res 12:77–88.

Hess JF, Casselman JT, Fitzgerald PG. 1996. Gene structure and cDNA sequence identify the beaded filament protein CP49 as a highly divergent type I intermediate filament protein. J Biol Chem 271:6729–6735.

Hirokawa N, Cheney RE, Willard M. 1983. Location of a protein of the fodrin-spectrin-TW260/240 family in the mouse intestinal brush border. Cell 32:953–965.

Hirokawa N, Heuser JE. 1981. Quick-freeze, deep-etch visualization of the cytoskeleton beneath surface differentiations of intestinal epithelial cells. J Cell Biol 91:399–409.

Hirokawa N, Tilney LG, Fujiwara K, Heuser JE. 1982. Organization of actin, myosin, and intermediate filaments in the brush border of intestinal epithelial cells. J Cell Biol 94:425–443.

Ireland M, Maisel H. 1984a. A cytoskeletal protein unique to lens fiber cell differentiation. Exp Eye Res 38:637–645.

Ireland M, Maisel H. 1984b. Phosphorylation of chick lens proteins. Curr Eye Res 3:961–968.

Ishii M, Miyazaki Y, Ohta S, Otsuki M, Goto Y. 1985. Three-dimensional structure of cytoskeletal system in human hepatocytes viewed by polyethylene-glycol-embedding method. Tohoku J Exp Med 147:47–63.

Keller TC, III, Conzelman KA, Chasan R, Mooseker MS. 1985. Role of myosin in terminal web contraction in isolated intestinal epithelial brush borders. J Cell Biol 100:1647–1655.

Keller TC, III, Mooseker MS. 1982. Ca++-calmodulin-dependent phosphorylation of myosin, and its role in brush border contraction in vitro. J Cell Biol 95:943–959.

Kuszak JR. 1995. The development of lens sutures. Prog Retin Eye Res 14:567–591.

Kuszak JR, Al-Ghoul KJ. 2002. A quantitative analysis of sutural contributions to variability in back vertex distance and scatter in rabbit lenses as a function of development, growth and age. Opt Vis Sci 79:193–204.

Kuszak JR, Brown HG. 1994. Embryology and anatomy of the crystalline lens. In: Albert DA, Jakobiec FA, editors. Principles and practice of ophthalmology: basic sciences. Philadelphia: W.B. Saunders Company. p 82–96.

Kuszak JR, Costello MJ. 2004. The structure of the vertebrate lens. In: Lovicu FJ, Robinson ML, editors. Development of the ocular lens. Cambridge: Cambridge University Press. p 71–118.

Kuszak JR, Mazurkiewicz M, Jison L, Madurski A, Ngando A, Zoltoski RK. 2006. Quantitative analysis of animal model lens anatomy: accommodative range is related to fiber structure and organization. Vet Ophthalmol 9:266–280.

Kuszak JR, Peterson KL, Herbert KL, Sivak JG. 1994. The interrelationship of lens anatomy and optical quality. II. Primate lenses. Exp Eye Res 59:521–535.

Kuszak JR, Sivak JG, Herbert KL, Scheib S, Garner W, Graff G. 2000. The relationship between rabbit lens optical quality and sutural anatomy after vitrectomy. Exp Eye Res 71:267–282.

Kuszak JR, Sivak JG, Weerheim JA. 1991. Lens optical quality is a direct function of lens sutural architecture. Invest Ophthalmol Vis Sci 32:2119–2129.

Kuszak JR, Zoltoski RK, Tiedemann CE. 2004. Development of lens sutures. Int J Dev Biol 48:889–902.

Lee A, Fischer RS, Fowler VM. 2000. Stabilization and remodeling of the membrane skeleton during lens fiber cell differentiation and maturation. Dev Dyn 217:257–270.

Lee A, Morrow JS, Fowler VM. 2001. Caspase remodeling of the spectrin membrane skeleton during lens development and aging. J Biol Chem 276:20735–20742.

Lu JY, Mohammed TA, Donohue ST, Al Ghoul KJ. 2008. Distribution of basal membrane complex components in elongating lens fibers. Mol Vis 14:1187–1203.

Luna EJ, Hitt AL. 1992. Cytoskeleton—plasma membrane interactions. 258:955–964.

Lux SE. 1979. Dissecting the red cell membrane skeleton. Nature, 281:426–429.

Massey-Harroche D, Mayran N, Maroux S. 1998. Polarized localizations of annexins I, II, VI and XIII in epithelial cells of intestinal, hepatic and pancreatic tissues. J Cell Sci 111 (Part 20):3007–3015.

Merdes A, Gounari F, Georgatos SD. 1993. The 47-kD lens-specific protein phakinin is a tailless intermediate filament protein and an assembly partner of filensin. J Cell Biol 123:1507–1516.

Mooseker MS. 1985. Organization, chemistry, and assembly of the cytoskeletal apparatus of the intestinal brush border. Annu Rev Cell Biol 1:209–241.

Mooseker MS, Pollard TD, Fujiwara K. 1978. Characterization and localization of myosin in the brush border of intestinal epithelial cells. J Cell Biol 79:444–453.

Nowak RB, Fischer RS, Zoltoski RK, Kuszak JR, Fowler VM. 2009. Tropomodulin1 is required for membrane skeleton organization and hexagonal geometry of fiber cells in the mouse lens. J Cell Biol 186:915–928.

Oka M, Kudo H, Sugama N, Asami Y, Takehana M. 2008. The function of filensin and phakinin in lens transparency. Mol Vis 14:815–822.

Pearl M, Fishkind D, Mooseker M, Keene D, Keller T, III. 1984. Studies on the spectrin-like protein from the intestinal brush border, TW 260/240, and characterization of its interaction with the cytoskeleton and actin. J Cell Biol 98:66–78.

Philp NJ, Nachmias VT. 1985. Components of the cytoskeleton in the retinal pigmented epithelium of the chick. J Cell Biol 101:358–362.

Quinlan R, Prescott A. 2004. Lens cell cytoskeleton. In: Lovicu FJ, Robinson ML, editors. Development of the ocular lens. Cambridge: Cambridge University Press. p 173–190.

Rafferty NS, Goossens W. 1978. Cytoplasmic filaments in the crystalline lens of various species: functional correlations. Exp Eye Res 26:177–190.

Rafferty NS, Scholz DL. 1989. Comparative study of actin filament patterns in lens epithelial cells. Are these determined by the mechanism of lens accommodation?Curr Eye Res 8:569–579.

Ramaekers F, Osborn M, Schmid E, Weber K, Bloemendal H, Franke W. 1980. Identification of the cytoskeletal proteins in the lens-forming cells, a special epithelioid cell type. Exp Cell Res 127:309–327.

Rodewald R, Newman SB, Karnovsky MJ. 1976. Contraction of isolated brush borders from the intestinal epithelium. J Cell Biol 70:541–554.

Rodman JS, Mooseker M, Farquhar MG. 1986. Cytoskeletal proteins of the rat kidney proximal tubule brush border. Eur J Cell Biol 42:319–327.

Rodriguez ML, Brignoni M, Salas PJ. 1994. A specifically apical sub-membrane intermediate filament cytoskeleton in non-brush-border epithelial cells. J Cell Sci 107 (Part 11):3145–3151.

Ross MH, Kaye GI, Pawlina W. 2003. Histology a text and atlas. 4th ed. Baltimore, MD: Lippincott Williams & Williams.

Salas PJ, Rodriguez ML, Viciana AL, Vega-Salas DE, Hauri HP. 1997. The apical submembrane cytoskeleton participates in the organization of the apical pole in epithelial cells. J Cell Biol 137:359–375.

Sandilands A, Prescott AR, Carter JM, Hutcheson AM, Quinlan RA, Richards J, Fitzgerald PG. 1995. Vimentin and CP49/filensin form distinct networks in the lens which are independently modulated during lens fibre cell differentiation. J Cell Sci 108 (Part 4):1397–1406.

Sandilands A, Prescott AR, Wegener A, Zoltoski RK, Hutcheson AM, Masaki S, Kuszak JR, Quinlan RA. 2003. Knockout of the intermediate filament protein CP49 destabilises the lens fibre cell cytoskeleton and decreases lens optical quality, but does not induce cataract. Exp Eye Res 76:385–391.

Schmitt-Graff A, Pau H, Spahr R, Piper HM, Skalli O, Gabbiani G. 1990. Appearance of alpha-smooth muscle actin in human eye lens cells of anterior capsular cataract and in cultured bovine lens-forming cells. Differentiation 43:115–122.

Shi Y, Barton K, De Maria A, Petrash JM, Shiels A, Bassnett S. 2009. The stratified syncytium of the vertebrate lens. J Cell Sci 122:1607–1615.

Shiels A, Bassnett S, Varadaraj K, Mathias R, Al-Ghoul K, Kuszak J, Donoviel D, Lillenberg S, Friedrich G, Zambrowicz B. 2001. Optical dysfunction of the crystalline lens in aquaporin-0 deficient mice. Physiol Genomics 7:179–186.

Shiels A, Mackay D, Bassnett S, Al Ghoul K, Kuszak J. 2000. Disruption of lens fiber cell architecture in mice expressing a chimeric AQP0-LTR protein. FASEB J 14:2207–2212.

Sivak JG, Herbert KL, Peterson KL, Kuszak JR. 1994. The interrelationship of lens anatomy and optical quality. I. Non-primate lenses. Exp Eye Res 59:505–520.

Sormunen R, Eskelinen S, Lehto VP. 1993. Bile canaliculus formation in cultured HEPG2 cells. Lab Invest 68:652–662.

Temm-Grove C, Helbing D, Wiegand C, Honer B, Jockusch BM. 1992. The upright position of brush border-type microvilli depends on myosin filaments. J Cell Sci 101 (Part 3):599–610.

Watanabe N, Tsukada N, Smith CR, Edwards V, Phillips MJ. 1991. Permeabilized hepatocyte couplets. Adenosine triphosphate-dependent bile canalicular contractions and a circumferential pericanalicular microfilament belt demonstrated. Lab Invest 65:203–213.

Weber K, Glenney JR, Jr. 1982. Microfilament-membrane interaction: the brush border of intestinal epithelial cells as a model. Philos Trans R Soc Lond B Biol Sci 299:207–214.

Woo MK, Lee A, Fischer RS, Moyer J, Fowler VM. 2000. The lens membrane skeleton contains structures preferentially enriched in spectrin-actin or tropomodulin-actin complexes. Cell Motil Cytoskeleton 46:257–268.